CSIRO PUBLISHING

Aust. J. Chem. **2014**, *67*, 626–635
http://dx.doi.org/10.1071/CH13483

Full Paper

Oxyhalogen–Sulfur Chemistry: Kinetics and Mechanism of Oxidation of *N*-Acetyl-L-methionine by Aqueous Iodine and Acidified Iodate

Kudzanai Chipiso,[A] *Wilbes Mbiya,*[A] *Moshood K. Morakinyo,*[A] *and Reuben H. Simoyi*[A,B,C]

[A]Department of Chemistry, Portland State University, Portland, OR 97207-0751, USA.
[B]School of Chemistry and Physics, University of KwaZulu-Natal, Westville Campus, Private Bag X54001, Durban 4000, Republic of South Africa.
[C]Corresponding author. Email: rsimoyi@pdx.edu

The use of *N*-acetyl-L-methionine (NAM) as a bio-available source for methionine supplementation as well as its ability to reduce the toxicity of acetaminophen poisoning has been reported. Its interaction with the complex physiological matrix, however, has not been thoroughly investigated. This manuscript reports on the kinetics and mechanism of oxidation of NAM by acidic iodate and aqueous iodine. Oxidation of NAM proceeds by a two electron transfer process resulting in formation of a sole product: *N*-acetyl-L-methionine sulfoxide (NAMS=O). Data from electrospray ionization mass spectrometry confirmed the product of oxidation as NAMS=O. The stoichiometry of the reaction was deduced to be $IO_3^- + 3NAM \rightarrow I^- + 3NAMS{=}O$. In excess iodate, the stoichiometry was deduced to be $2IO_3^- + 5NAM + 2H^+ \rightarrow I_2 + 5NAMS{=}O + H_2O$. The reaction between aqueous iodine and NAM gave a 1 : 1 stoichiometric ratio: $NAM + I_2 + H_2O \rightarrow NAMS{=}O + 2I^- + H^+$. This reaction was relatively rapid when compared with that between NAM and iodate. It did, however, exhibit some auto-inhibitory effects through the formation of triiodide (I_3^-) which is a relatively inert electrophile when compared with aqueous iodine. A simple mechanism containing 11 reactions gave a reasonably good fit to the experimental data.

Manuscript received: 12 September 2013.
Manuscript accepted: 6 November 2013.
Published online: 17 January 2014.

Introduction

Organosulfur compounds play a major role in synthetic, analytical, and medicinal chemistry. Oxidations of these organosulfur compounds appear to be involved in many cellular functions including protection of the cell from oxidative damage.[1] Sulfur-containing amino acids play an important role in antioxidant defence in humans.[2] In the physiological environment sulfur is found in many amino acids, making it the third most abundant micro-mineral on the basis of total bodyweight in humans.[3] Methionine is an essential amino acid that is required for protein synthesis as well as other biochemical processes and cell proliferation.[4] Methionine, like cysteine, can act as an antioxidant and as a key component in metabolism regulation. *N*-Acetyl-L-methionine (NAM) is a derivative of the amino acid methionine with an acetyl group attached to the nitrogen atom. NAM is effectively deacetylated by acyclase 1 (ACY1; EC 3.5.1.14) which is expressed in a wide range of human tissues including the brain.[5,6] Although the deacetylating enzyme has been known for years, it remains unclear which enzyme is responsible for acetylation of methionine. The current theory suggests that free NAM is the direct result of degradation of acetylated proteins but there are no previous documented reports on acetylation of free methionine.[7] NAM has long been recognized as a bio-available source for the essential amino acid methionine.[8] Considerable evidence from the literature has suggested that NAM can replace methionine as an essential amino acid in the human diet.[9] The two compounds are nutritionally and metabolically equivalent. Supplemental methionine may undergo a chemical modification during processing, producing a disagreeable odour.[10] However, the protection of the L-acetyl-methionine α-amino group with an *N*-acetyl group prevents the Strecker degradation, enhancing the potential of NAM as a food additive in place of methionine.[11,12] NAM is a powerful antioxidant capable of acting as an antitoxin to liver toxicity from bromobenzene.[13] It has been found to stabilize liver glutathione (GSH) levels after depletion as a result of acetaminophen toxicity and hence prevent liver toxicity.[14] Thus it is also involved in the production of GSH, cysteine, and taurine, all of which help to eliminate toxins from the body. A combination of anticancer therapy involving the infusion of NAM and *N*-acetyl-L-selenomethionine (NASeM) shows promising results in targeted anticancer therapy and thus pharmacokinetic evaluation of the data is currently underway.[15] Interestingly, although both NAM and methionine are required for growth, excess dietary quantities have been shown to result in progressive decreases in weight gain, and have also caused comparable hypertrophy of the spleen and increases in spleen iron levels.[16]

Despite the importance of NAM, few studies on its metabolism have been carried out. Several of these studies have

concentrated on comparing and evaluating the nutritional value of methionine and NAM. Our research interest has largely focussed on the kinetics and mechanistic studies of these two compounds. The sulfur centres of the organosulfur compounds are highly susceptible to oxidation by various biological oxidants such as H_2O_2 and HOCl, which are formed in neutrophils during inflammation and have bactericidal effects.[17–20] The rate of methionine acetylation to NAM has been found to be very high in the brains of mice and humans.[7]

Here, the oxidation of NAM by aqueous iodine and acidic iodate is reported.

Experimental

Materials

The following reagent grade chemicals were used without further purification: sodium iodate, perchloric acid (70–72 %), sodium iodide, iodine, sodium perchlorate, soluble starch, sodium thiosulfate (Fisher), NAM (Sigma). Iodine solutions, being volatile, were kept capped and standardized spectrophotometrically before each set of experiments. Stock solutions of NAM were prepared just before use.

Methods

The rapid reactions of NAM with iodine were followed on a Hi-Tech Scientific SF61-DX2 double-mixing stopped-flow spectrophotometer. These reactions were monitored by following the consumption and formation of iodine at 460 nm ($\varepsilon = 770\,M^{-1}\,cm^{-1}$). NAM has no absorbance in the visible region, while aqueous iodine has an isolated peak at 460 nm (see Fig. 1). This absorbance reading could also be used for analytical determination of aqueous iodine. Slower reactions involving oxidation of NAM by acidified iodate were monitored on a conventional Perkin–Elmer Lambda 25 UV-vis spectrophotometer.

All kinetics experiments were performed at 25.0 ± 0.5°C and at an ionic strength of 1.0 M ($NaClO_4$). All solutions were prepared using doubly-distilled deionized water from a Barnstead Sybron Corporation water purification unit capable of producing both distilled and deionized water (Nanopure).

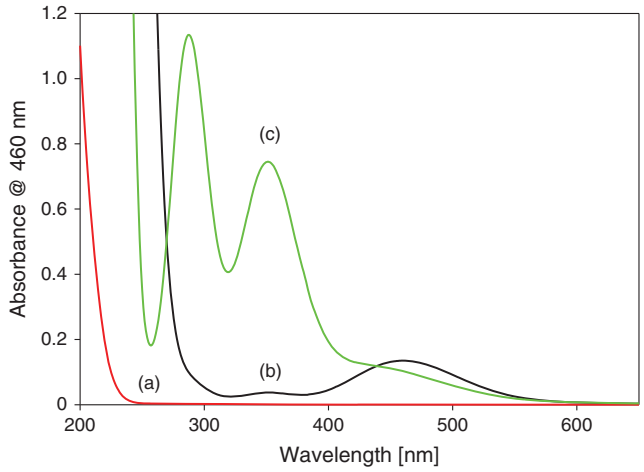

Fig. 1. UV-vis spectra of (a) *N*-acetyl-L-methionine (NAM), (b) iodine, and (c) the product of NAM and acidified iodate. Iodine absorbs at 460 nm. However, the iodine/triiodide mixture results in two additional peaks observed at 286 and 353 nm. The peak at 460 nm becomes an isosbestic point for iodine and triiodide. Since NAM does not absorb in the UV-vis region and there was no interference from iodine/triiodide; the peak at 460 nm was used to quantify iodine concentrations.

Electrospray ionization mass spectrometry (ESI-MS) of the product solutions was performed using a Thermo Scientific LTQ-Orbitrap Discovery mass spectrometer (San Jose, CA) equipped with an electrospray ionization source operated mostly in the negative mode.

Results and Discussion

Stoichiometry

For a fixed concentration of acidified NAM (0.001 M), a series of varying concentrations of excess iodate were added and solutions left to stand overnight. The excess oxidizing power left after total consumption of NAM was determined iodometrically by adding excess iodide and titrating the liberated iodine against standard thiosulfate with starch as indicator. The volume of thiosulfate was then plotted against initial iodate concentrations (see Fig. 2). The linear plot is then extrapolated to the iodate axis to derive the concentration of iodate needed to just oxidize NAM with no iodate left to produce iodine from the Dushman reaction.[22] Fig. 2 shows an intercept value of 0.32×10^{-3} M iodate which represents the stoichiometric amount of iodate needed to consume an equal volume of 0.001 M NAM. This suggests a 1 : 3 stoichiometry of iodate to NAM:

$$IO_3^- + 3NAM \rightarrow 3NAMS{=}O + I^- \qquad (1)$$

where NAMS=O is *N*-acetyl-L-methionine sulfoxide. The 1 : 3 ratio indicates a two-electron oxidation of the sulfur centre in NAM to either the sulfenic acid or the sulfoxide in which the methionine skeletal structure stays intact (see Scheme 1). ^{1}H NMR spectra shown in Fig. 3 also confirm the formation of a single product, the sulfoxide. Oxidation of the sulfur atom to the sulfoxide renders the sulfur atom chiral, which would show a complex multiplet for the now diastereotopic methylene protons next to it. The two sets of methylene protons thus effectively coalesce. The proton on the asymmetric carbon centre is quite removed from the oxidized sulfur centre and is not expected to be altered much by the oxidation. The slight difference observed between products derived from aqueous iodine and acidic iodate arises from the fact that iodate oxidations occur, and can only be carried out, at low pH. The sulfur centre ceases to be asymmetric if it is oxidized further to the sulfone.

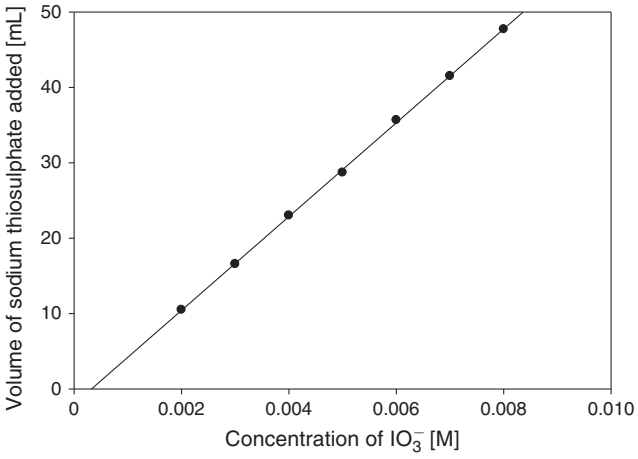

Fig. 2. Titration results of oxidation of *N*-acetyl-L-methionine (NAM) in excess iodate conditions. The intercept on the [IO_3^-] axis is 0.00032 M suggesting a 1 : 3 (iodate to NAM) stoichiometric ratio. $[NAM]_0 = 1.0 \times 10^{-3}$ M, $[H^+]_0 = 5.0 \times 10^{-3}$ M.

Sulfenic acids are known to be very unstable and are rarely isolated, except in sterically hindered molecules.[23–25] It is not anticipated that NAM will be able to stabilize a sulfenic acid. ESI-MS data shown in Fig. 4 indicates the formation of a single product: NAMS=O. No other product was observed except for the addition of a single oxygen onto the sulfur atom of the thioether. The spectrum in Fig. 4 was obtained in a slight excess of acidic iodate. It also shows a strong peak for iodide and a weaker peak for the unreacted iodate. In excess iodate, the iodide produced in Eqn 1 asserts the Dushman[26–28] reaction to form iodine:

$$IO_3^- + 5I^- + 6H^+ \rightarrow 3I_2 + 3H_2O \qquad (2)$$

Thus the overall reaction stoichiometry in excess iodate is a combination of Eqns 1 and 2 which consumes all the iodide formed in Eqn 1:

$$2IO_3^- + 5NAM + 2H^+ \rightarrow I_2 + 5NAMS{=}O + H_2O \qquad (3)$$

The reaction was followed by observing the formation of iodine, which was only possible in excess iodate, and thus the stoichiometry in Eqn 3 is the relevant stoichiometry during our study of this reaction. Fig. 5 shows the ESI mass spectrum derived from the NAM–iodate reaction at its stoichiometric ratio of 3 : 1. The spectrum was acquired before the reaction had proceeded to completion, and thus still shows peaks for the substrate and iodate at *m/z* 191.01 and 174.89 respectively. Iodine formation was dependent on initial concentrations of NAM, and the amount of iodine formed was exactly 20 % of the initial concentration of NAM. Assuming an oxidant to reductant ratio, $R = [IO_3]_0/[NAM]_0 > 0.40$; the stoichiometry in Eqn 3 was followed. For values of $0.33 < R < 0.40$; although molecular iodine was formed, there was not enough iodate to satisfy

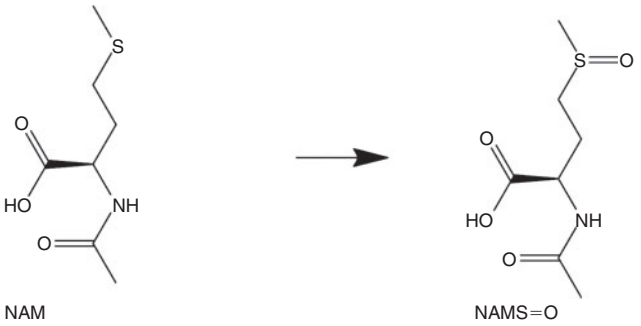

Scheme 1. *N*-Acetyl-L-methionine (NAM) is oxidized to *N*-acetyl-L-methionine sulfoxide (NAMS=O).

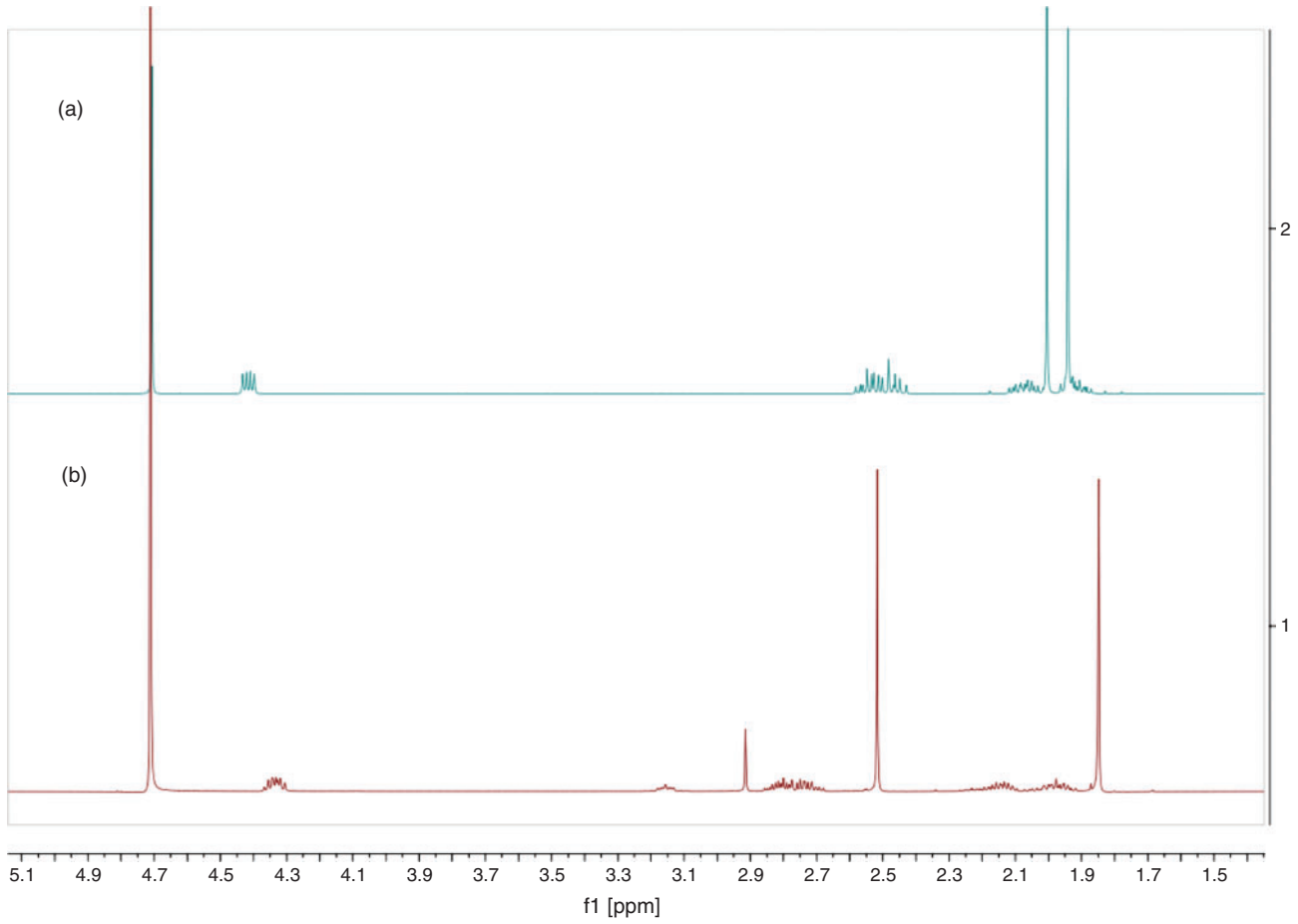

Fig. 3. ^{1}H NMR spectra of (a) *N*-acetyl-L-methionine (NAM) and (b) the oxidation product of NAM from acidic iodate/iodine which is *N*-acetyl-L-methionine sulfoxide. It shows a shift of the S-methyl protons downfield from 2.00 to 2.52 ppm and the S-methylene protons from 2.50 to 2.78 ppm after formation of the sulfoxide. The formation of the sulfoxide makes the sulfur centre chiral thus making the methylene protons next to the sulfur centre diastereotopic, hence the complex multiplet. As expected the proton on the asymmetric carbon at 4.35 ppm is barely affected by the sulfoxide formation. The peak at 2.91 ppm is due to the formation of HDO.[21]

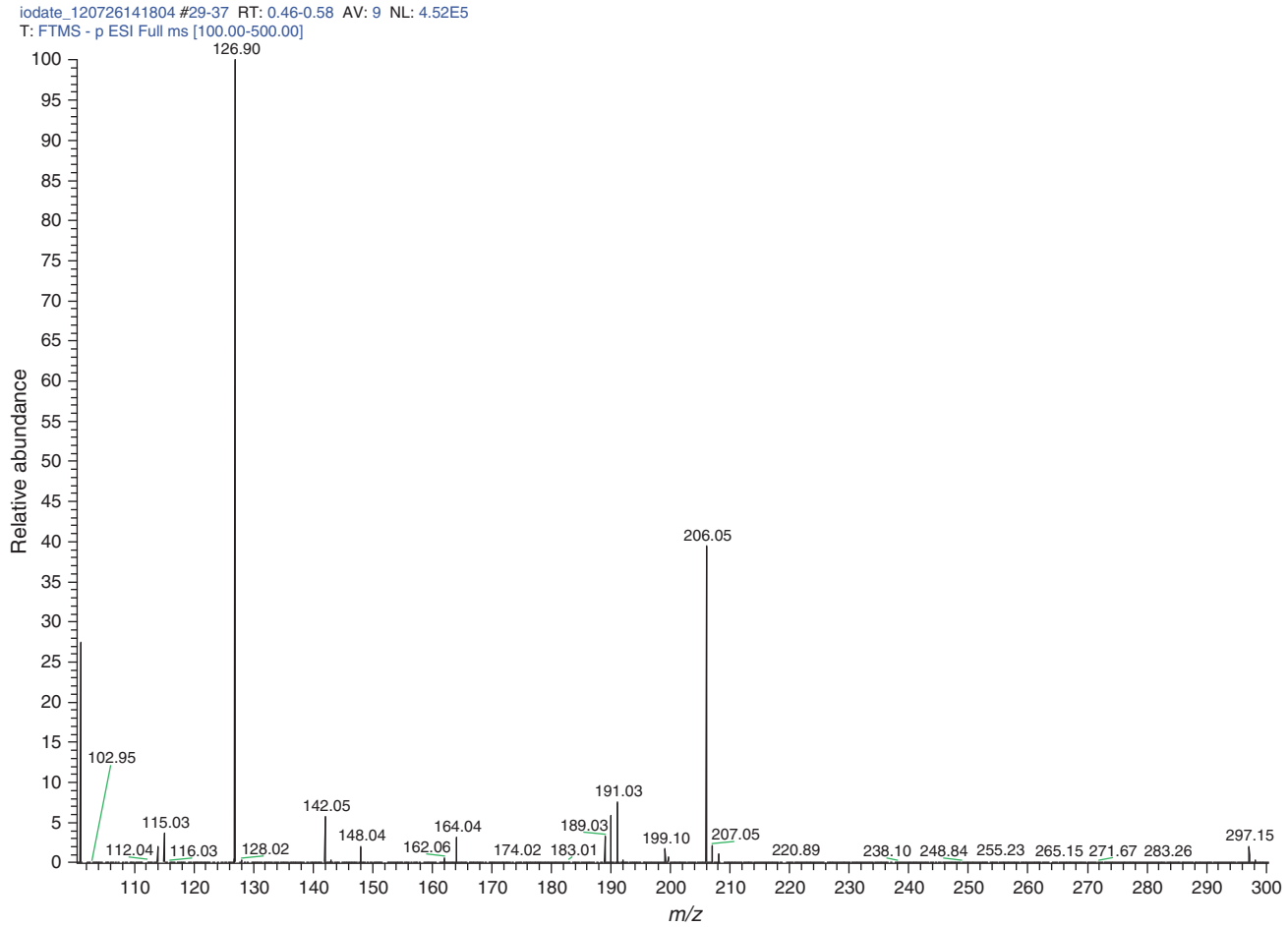

Fig. 4. Negative mode electrospray ionization mass spectrum of a stoichiometric 1 : 1 ratio of [*N*-acetyl-L-methionine (NAM)] : [I_2] using 50 : 50 methanol/water as solvent. Only two peaks are observed, one for iodide at *m*/*z* 126.90 and the sulfoxide product at *m*/*z* 206.05.

Eqn 3. An equally relevant reaction in acidic iodate–NAM mixtures is the direct reaction of aqueous iodine with NAM. Its stoichiometry, rate, and viability will determine the overall reaction dynamics, especially with respect to formation of iodine. As mentioned above, the ESI-MS spectrum of an aqueous iodine–NAM mixture (Fig. 4) only gives peaks for the sulfoxide and for iodide. Through a combination of spectrophotometric and iodometric techniques, the stoichiometry of the I_2–NAM reaction was deduced to be 1 : 1.

$$I_2 + NAM + H_2O \rightarrow NAMS{=}O + 2I^- + 2H^+ \qquad (4)$$

Reaction Kinetics

Fig. 6 shows successive UV-vis spectra of the reaction mixture taken every 70 s. While the initial spectrum (reactants: NAM, IO_3^-, and H^+) has no peaks in the visible region, after a short quiescent period, peaks emerge at 355 and 460 nm. These are attributed to triiodide and the isosbestic point of iodine/triiodide respectively. Figs 7–9 show that the reaction does not have a sharp induction period with respect to iodine formation. Iodine formation is observed almost instantly upon reaction commencement.

Formation of iodine is derived from the Dushman reaction:[22,26,27] this requires iodide which has to be derived from Eqn 1. One would expect a time lag, from reaction commencement, before formation of iodine is observed. Iodine formation, however, commences almost immediately (albeit, slowly at first and increasing in rate of formation). Final observed iodine concentrations are based on the stoichiometry of Eqn 3 as in Fig. 7 where initial NAM concentrations are varied consistently at $R > 0.40$. Increasing iodate concentrations increased the rate of formation of iodine, but did not alter the final amount of iodine formed for all solutions with $R > 0.40$ (Fig. 8). The same was observed for acid variation experiments shown in Fig. 9. The direct reaction of iodine with NAM was relatively faster than the iodate oxidation of NAM, but not overwhelmingly so; such that the rates of these two sets of reactions were comparable. This can explain the lack of an induction period in iodine formation for reactions run in excess iodate.

Kinetics of the I_2–NAM Reaction

Fig. 10 shows the dependence of the reaction on NAM concentrations. The reaction showed typical bimolecular kinetics in which it starts off rapidly and slows down dramatically. This could also be indicative of a self-inhibiting reaction. The initial part of the reaction was first order in $[NAM]_0$. A plot of initial rate of reaction versus $[NAM]_0$ gave a straight line, indicating first order kinetics in [NAM]. Data shown in Fig. 10 give a bimolecular rate constant of $5.23 \pm 0.81\ M^{-1}\ s^{-1}$. Fig. 11 shows the iodine dependence on the rate of reaction; this also shows initial bimolecular kinetics, and a plot of initial rate versus iodine concentrations showed first order dependence in

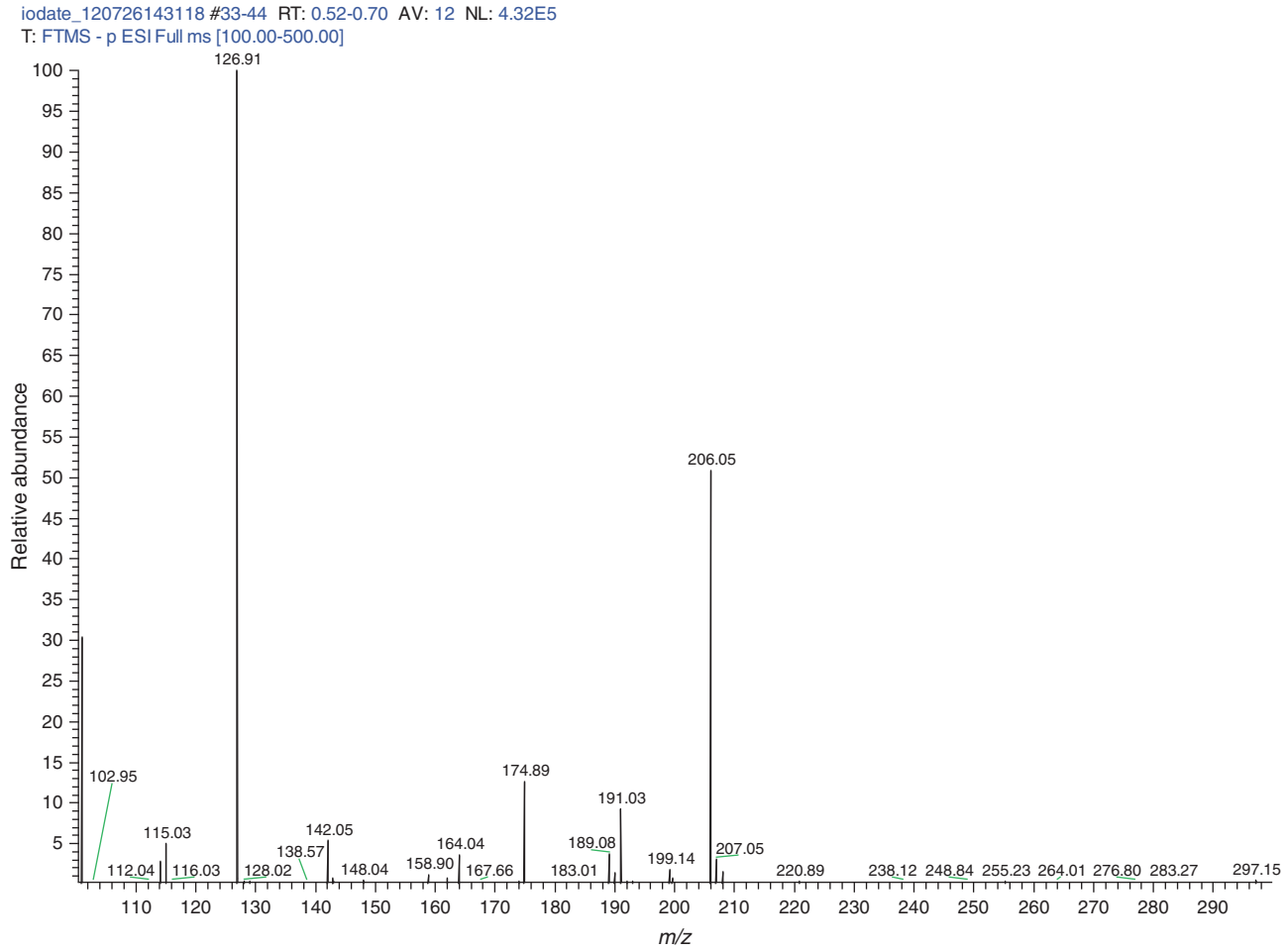

Fig. 5. Negative mode electrospray ionization mass spectrum of a stoichiometric 3 : 1 ratio of [NAM] : [IO_3^-] using 50 : 50 methanol/water as solvent. The two major peaks belong to the sulfoxide product at *m/z* 206.05 and iodide at 126.91. Residual iodate can be seen at *m/z* 174.89. The spectrum was taken before the reaction had reached completion.

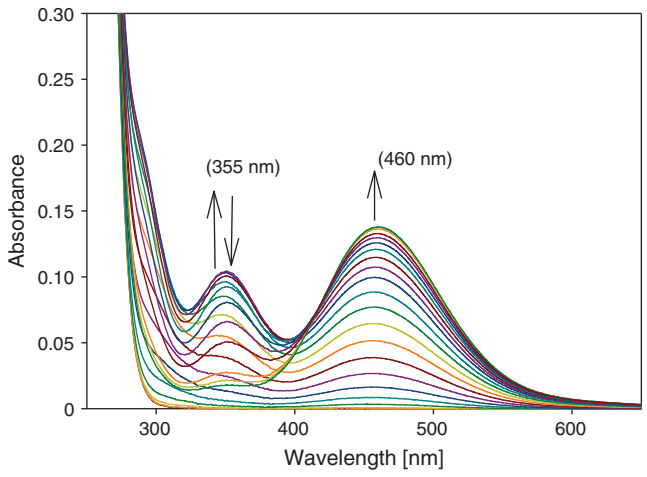

Fig. 6. Spectroscopic changes observed every 70 s. [*N*-acetyl-L-methionine (NAM)]$_0$ = 0.001 M, [IO_3^-]$_0$ = 0.02 M, and [H^+]$_0$ = 0.05 M.

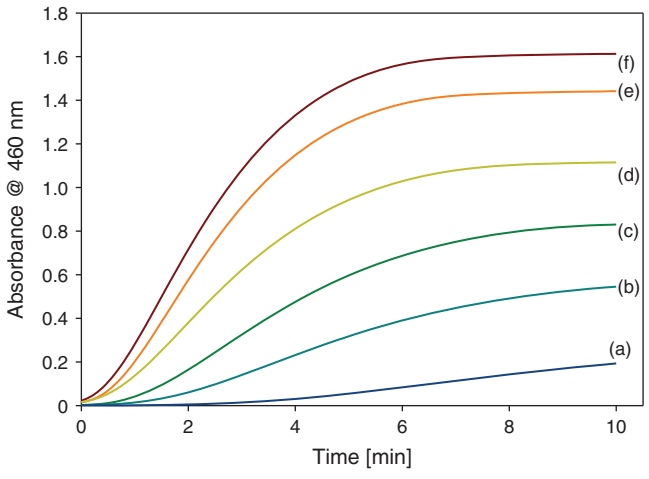

Fig. 7. Absorbance traces for *N*-acetyl-L-methionine (NAM) variation in its oxidation by iodate. [IO_3^-]$_0$ = 0.06 M, [H^+]$_0$ = 0.02 M, [NAM]$_0$ = (a) 0.002, (b) 0.004 (c) 0.006, (d) 0.008, (e) 0.010, and (f) 0.012 M. The traces show an increase in absorbance as the concentration of NAM is increased from (a)–(f).

iodine with a derived rate constant statistically equivalent to the one derived from data in Fig. 10.

Fig. 12 shows that the product, iodide, inhibits the NAM–I_2 reaction. This is the source of the observed auto-inhibition. There was no simple relationship derivable from the data in Fig. 12 linking the rate of reaction with initial iodide concentrations. A plot of the inverse of initial reaction rate versus iodide concentrations shown in Fig. 13 does show a linear relationship.

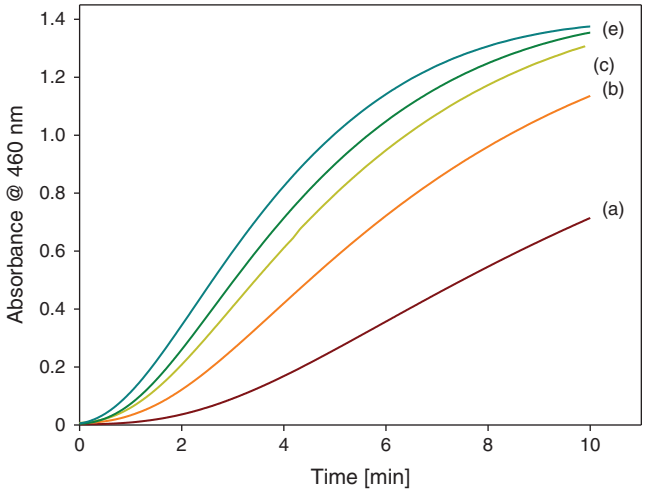

Fig. 8. Absorbance traces of the reaction between *N*-acetyl-L-methionine (NAM) and IO_3^- showing the effect of progressively increasing iodate concentration. In excess iodate the final iodine amount reaches a maximum determined by the NAM concentration. All these experimental runs gave the same final iodine concentrations.

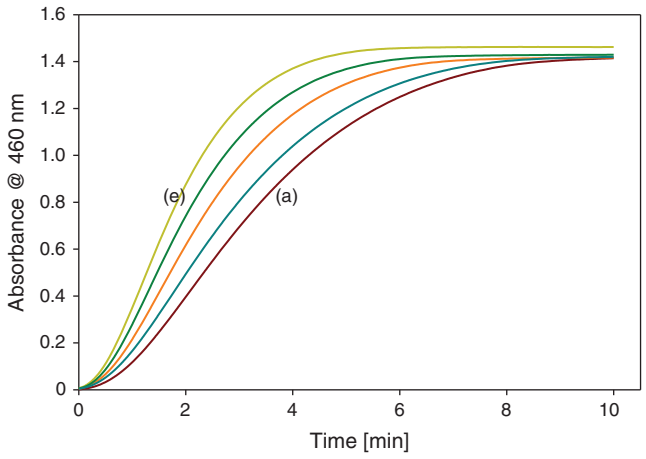

Fig. 9. The effect of varying acid concentration for the reaction runs in excess iodate. Acid is a catalyst in this reaction. [*N*-acetyl-L-methionine (NAM)]$_0 = 0.01$ M, [IO_3^-] = 0.05 M, varied [H^+] = (a) 0.002, (b) 0.003, (c) 0.004, (d) 0.005 M, and (e) 0.006 M.

Mechanism

Acidic iodate oxidations have been extensively studied and standard oxyiodine kinetics have been well established which involve the initiation reaction of the Dushman reaction as being dominant.[27–29] This involves protonation of iodate to form iodic acid which is then attacked by the nucleophilic iodide species to form an adduct which breaks up in a rate-determining step to form the reactive oxyiodine species HOI and HIO_2:

$$H^+ + IO_3^- \rightleftarrows HIO_3 \quad (5)$$

$$HIO_3 + I^- \rightleftarrows HI_2O_3^- \quad (6)$$

$$HI_2O_3^- + H^+ \rightarrow HOI + HIO_2 \text{ (rate-determining step)} \quad (7)$$

Since Eqn 7 is the rate-determining step, the rate of the reaction will be $k_0[IO_3^-][I^-][H^+]^2$. Other laboratories have derived

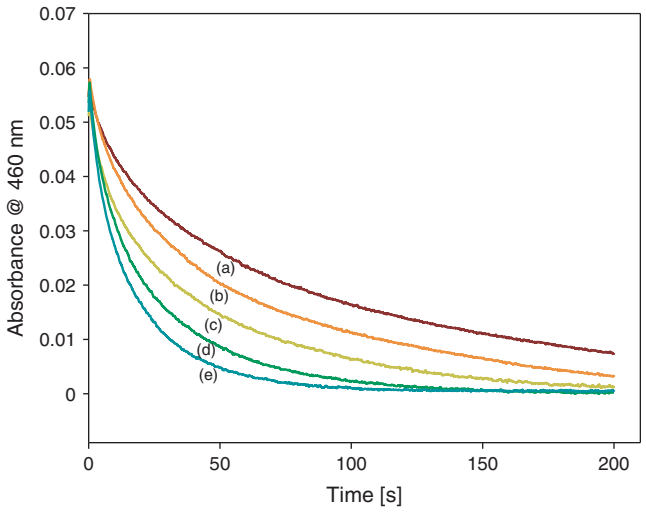

Fig. 10. Traces showing variation of *N*-acetyl-L-methionine (NAM) concentration with constant iodine concentration. $[I_2]_0 = 1.0 \times 10^{-4}$ M and varied [NAM]$_0$ = (a) 0.00039, (b) 0.00078, (c) 0.0016, (d) 0.0062, and (e) 0.025 M.

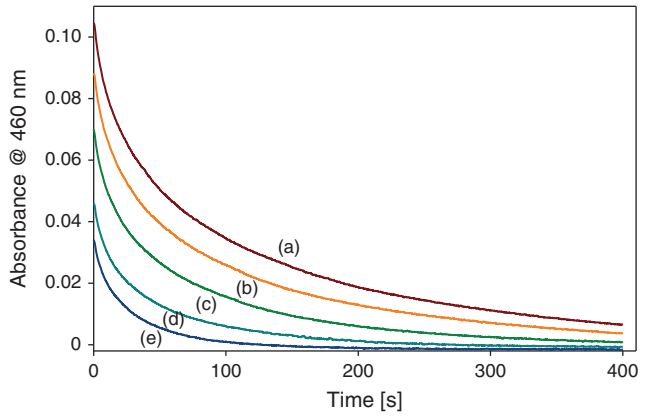

Fig. 11. Traces showing effect of progressively increasing iodine concentration on the oxidation of [*N*-acetyl-L-methionine (NAM)]$_0 = 0.001$ M and $[I_2]_0$ = (a) 1.5×10^{-4}, (b) 1.2×10^{-4}, (c) 9.0×10^{-5}, (d) 7.0×10^{-5}, (e) 5.0×10^{-5} M.

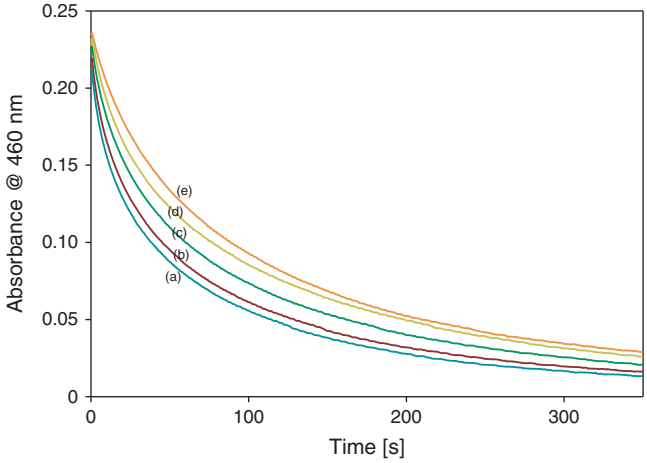

Fig. 12. (a) Effect of deliberately adding iodide (product of reaction) on the rate of reaction. [*N*-acetyl-L-methionine (NAM)]$_0 = 0.01$ M, $[I_2]$ = 0.0003 M, and [I^-] = (a) no added iodide, (b) 0.00005, (c) 0.0001, (d) 0.0002, and (e) 0.0003M.

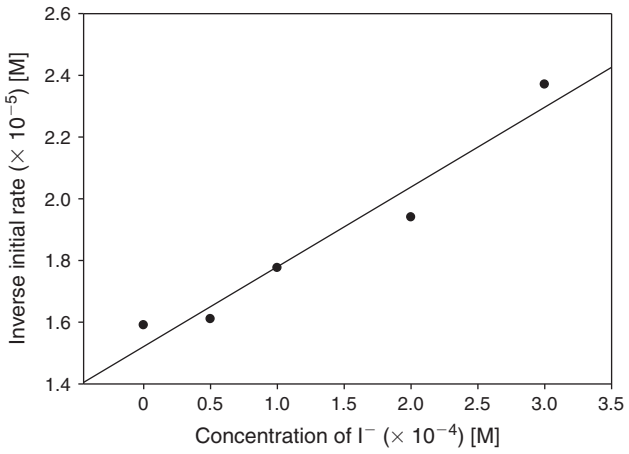

Fig. 13. The inverse plot of the initial rate and iodide concentrations in Fig. 12. A positive intercept and positive slope indicates at least two oxidizing species.

more complex reaction kinetics for the Dushman reaction which involve a two-term rate law.[28] The second pathway involves a further pre-equilibrium step involving the $HI_2O_3^-$ complex:

$$HI_2O_3^- + H^+ \rightleftharpoons H_2I_2O_3 \qquad (8)$$

The $H_2I_2O_3$ complex is involved in a rapid dehydration equilibrium:

$$H_2I_2O_3 \rightleftharpoons I_2O_2 + H_2O\,(\text{rapid}) \qquad (9)$$

This then brings into the mechanistic scheme a new rate-determining step involving iodide:

$$I_2O_2 + I^- \rightarrow I_3O_2^-\,(\text{rate-determining step}) \qquad (10)$$

A series of rapid steps then occur to produce iodine and water:

$$I_3O_2^- + 6I^- + 4H^+ \rightarrow 3I_3^- + 2H_2O \qquad (11)$$

Combining both pathways, the rate of reaction becomes:

$$\text{Rate} = k_0[IO_3^-][I^-][H^+]^2 + k_1[IO_3^-][I^-]^2[H^+]^2 \qquad (12)$$

Eqn 10 is enhanced by high iodide environments, culminating in formation of triiodide (I_3^-). At low iodide conditions Eqn 11 gives predominantly aqueous molecular iodine:

$$I_3O_2^- + 3I^- + 4H^+ \rightarrow 3I_2 + 2H_2O \qquad (13)$$

Modelling the kinetics of the reaction while including the second term in Eqn 12 did not improve the fit. The volume of the second term is negligible under the conditions utilized in this study of the stoichiometry of Eqn 3 since all iodide produced in the stoichiometry of Eqn 1 is consumed through the Dushman reaction, and is never high enough to make the second term in Eqn 12 relevant. Thus this pathway was assumed to be negligible.

Mechanism of the I_2–NAM Reaction

Fig. 14 shows that iodide catalyzes the reaction, at least with respect to formation of iodine: its rate and its early onset.

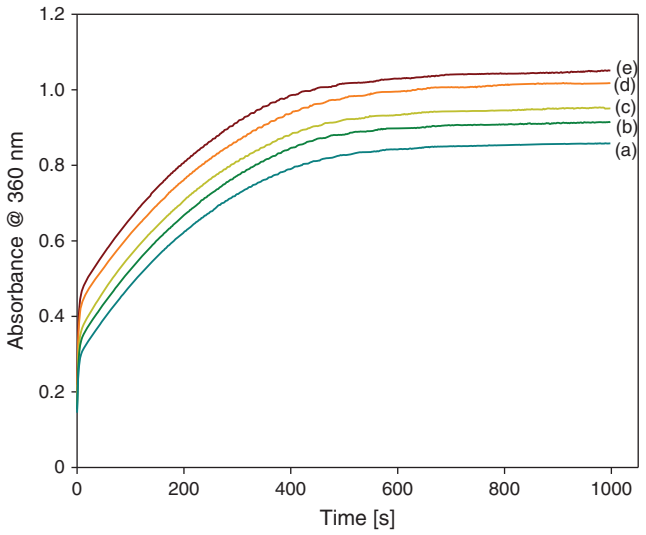

Fig. 14. Absorbance traces, showing the effect of deliberately adding iodide to the *N*-acetyl-L-methionine (NAM) oxidation by iodate. A very fast rate of reaction is initially observed for all concentrations: $[NAM]_0 = 0.004$ M, $[H^+]_0 = 0.02$ M, $[IO_3^-] = 0.06$ M, and $[I^-]$ = (a) 0.0010, (b) 0.0011, (c) 0.0012, (d) 0.0013, and (e) 0.0014 M.

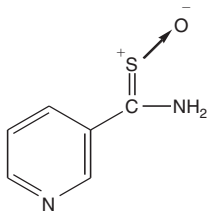

Thionicotinamide S-oxide

Chart 1.

However, Fig. 12 shows that iodide inhibits the direct oxidation of NAM by iodine. The initial step of the NAM–I_2 reaction is an electrophilic attack by iodine on the nucleophilic thiol centre (Eqn 14) followed by a hydrolysis (Eqn 15) to a very unstable intermediate which immediately rearranges to give the sulfoxide:

$$NAM + I_2 \rightleftarrows [NAMS{-}I]^+ + I^- \qquad (14)$$

$$[NAMS{-}I]^+ + H_2O \rightarrow [NAMS{-}OH]^+ + H^+ + I^- \qquad (15)$$

The electrophilic species formed in Eqn 15 (the positively charged sulfenic acid) can only be stabilized as an S-oxide as has been observed in thionicotinamide S-oxide (Chart 1).[30]

Without large stearically hindering, electron-donating groups, a sulfenic acid will not be formed.[23,24] The sulfoxide is then formed from the formation of the S=O double bond, with a concomitant expulsion of a proton.

$$[NAMS{-}OH]^+ \rightarrow NAMS{=}O + H^+ \qquad (16)$$

No further oxidation occurs past this sulfoxide. Sulfoxides with electron-donating groups on either side of the sulfur atom are known to be stable. Methionine sulfoxide can be purchased as a normal analytical reagent from chemical vendors and is a

well known bioactive molecule.[19,31–33] The overall stoichiometry of this reaction (Eqn 4) introduces iodide ions into the reaction medium. Iodide is known to form an equilibrium mixture with aqueous iodine to form triiodide:[34,35]

$$I_2 + I^- \rightleftarrows I_3^- \quad (17)$$

Initial attack (Eqn 14) is an electrophilic attack by molecular iodine. Triiodide, on the other hand, is a nucleophile and would undergo Eqn 14 at a much slower rate than molecular iodine. This will inhibit the reaction, and this inhibition intensifies as the reaction proceeds and more iodide is formed. If one assumes, in the extreme case, that triiodide is inert, then the rate of the I_2–NAM reaction is given by:

$$\text{rate} = \frac{k_2[I_2]_0[\text{NAM}]_0}{1 + K_{eq}[I^-]} \quad (18)$$

The '0' subscripts denote initial concentrations. One can re-write Eqn 18 in a linear form as follows:

$$\frac{1}{\text{rate}} = \frac{1}{k_2[I_2]_0[\text{NAM}]_0} + \frac{K_{eq}[I^-]_0}{k_2[I_2]_0[\text{NAM}]_0} \quad (19)$$

A plot of the modulus of the inverse of the rate versus added iodide concentration should give a straight line that should deliver a value of k_2 from the intercept and a value for K_{eq}, if indeed I_3^- was inert. The slope of the plot should deliver the bimolecular rate constant between iodine and NAM. In the limit of high initial iodide concentrations, the second term in Eqn 19 dominates. With no iodide ions initially added to the reaction mixture, Eqn 19 reverts to a pure bimolecular reaction that should deliver a value for k_2. This value can be checked against the one generated from the initial rate data from Figs 10 and 11. This treatment deduced k_2 to be 5.65 M^{-1} s^{-1}. This value is not very different from that determined from the initial rate studies of 5.23 M^{-1} s^{-1}. If we assume this rate constant, we can utilise the slope of the graph to determine the K_{eq} of the I_2/I_3^- equilibrium. If the value determined is lower than the literature value[34] of 770 M^{-1}, this would indicate that I_3^- is not totally inert, and does contribute, albeit at a lower effective rate. A sharp slope in the plot indicates a strong iodide effect and a larger discrepancy in the reactivities of I_2 versus I_3^-. The plot in Fig. 13 deduced a value of $K_{eq} = 478\ M^{-1}$ (no error bars available for this value, unless several iodide dependence plots had been performed at various combinations of initial reagent concentrations). This deduced value for K_{eq} indicates a strong contribution to oxidation of NAM from I_3^-.

Overall Reaction Dynamics

The reaction of molecular iodine with NAM is sluggish enough such that it is unable to mop up all the iodine generated through the Dushman reaction. Hence iodine formation commences almost as soon as acidic iodate and NAM are mixed together. Iodate is inert in low acid environments. Highly acidic environments inhibit Eqn 14, the direct reaction between NAM and I_2, by protonating the nucleophilic sulfur centre of the thioether. The reaction initiation itself, in the absence of added iodide, is through a general reaction of iodic acid with the thioether, generating a cascade of reactive oxyiodine species which will promote the reaction's progress. One can write the following series of reactions (Eqns 20–22), which lead to the initial accumulation of iodide and subsequent formation of iodine. We can represent NAM as $RSCH_3$, a methyl thioether.

$$HIO_3 + RSCH_3 \rightarrow HIO_2 + RSOCH_3 \quad (20)$$

$$HIO_2 + RSCH_3 \rightarrow HOI + RSOCH_3 \quad (21)$$

$$HOI + RSCH_3 \rightarrow H^+ + I^- + RSOCH_3 \quad (22)$$

Accumulation of I^- from Eqns 20–22 then transfers the rate-determining step to Eqn 23:

$$IO_3^- + H^+ + I^- \rightleftarrows HIO_2 + HOI \quad (23)$$

Eqn 23 is the initiation reaction for the Dushman reaction in low iodide conditions, with iodine subsequently generated in a single reaction:[36]

$$HOI + I^- + H^+ \rightarrow I_2 + H_2O \quad (24)$$

Reduction of iodine by NAM (Eqn 4) generates iodide which inhibits its further reduction, but catalyzes the reaction that forms iodine (Eqn 23). Coupled with the protonation of the sulfur centre, this explains the almost instant iodine formation observed.

Reaction Modelling

The whole reaction scheme is compiled in the reactions shown in Table 1. It is a simple 11-reaction scheme that does not assume complete inertness of the triiodide (the discrepancy in K_{eq} values obtained from our experimental data and literature values indicates some activity by triiodide), but the assumed rate constant was much less than that assumed for aqueous iodine. The first five reactions are standard iodine and oxyiodine reactions, and their kinetics values were sourced from literature values.[22,27–29] Reaction M6, the association/dissociation of iodic acid, was derived from silver iodate solubility studies of Naidich and Ricci.[37] Although a dissociation constant for HIO_3 of 0.163 was derived, it was not easy to extrapolate to our conditions (pH and ionic strength). Work by Li and Lo[38] deduced a slightly lower value of 0.154, but values as high as 0.470 have also been reported.[39] However, since it is a protolytic process, reaction rates were assumed to be nearly diffusion-controlled, in both directions, while adhering to the acid dissociation constant.

Reactions M7–M9 represent the initiation cascade of reactions needed to generate the reactive species through accumulation of iodide. The normally believed theory that iodate solutions always have high enough iodide concentrations, $\sim 10^{-6}$ M, to initiate Eqn 23 could not explain the almost instant production of iodine a few seconds after mixing reaction solutions. Thus, in simulating the global reaction dynamics, the most important kinetics parameter is k_{M7}; the initiation reaction that starts the iodide formation cascade. The value adopted for this parameter determined the rate of formation of aqueous iodine. Kinetic parameters for reactions M8 and M9 are not relevant for as long as they are faster than the rate constant for M7. Reactions M9 and M10 involve oxidation of NAM by HOI and I_2 respectively. Reaction M9 involves an oxygen atom transfer while M10 is an electrophilic attack followed by a hydrolysis. In this mechanism, we made $k_{M9} > k_{M10}$. Overall, this did not affect the simulations because of the low HOI

Table 1. Complete compilation of the reactions involved in the overall scheme for the oxidation of *N*-acetyl-L-methionine (NAM) by aqueous iodine and acidic iodate

Number	Reaction[A]	k_f, k_r^B
M1	$IO_3^- + I^- + 2H^+ \rightleftharpoons HIO_2 + HOI$	2.8, 1.44×10^3
M2	$HIO_2 + I^- + H^+ \rightleftharpoons 2HOI$	2.1×10^8, 90
M3	$HOI + I^- + H^+ \rightleftharpoons I_2 + H_2O$	3.1×10^{12}, 2.2
M4	$IO_3^- + HOI + H^+ \rightleftharpoons 2HIO_2$	8.6×10^2, 2.00
M5	$I_2 + I^- \rightleftharpoons I_3^-$	6.2×10^9, 8.5×10^6
M6	$IO_3^- + H^+ \rightleftharpoons HIO_3$	5.0×10^9, 1.25×10^9
M7	$HIO_3 + RSR + H^+ \rightarrow HIO_2 + NAMS{=}O + H^+$	3.8
M8	$HIO_2 + RSR \rightarrow HOI + NAMS{=}O$	50
M9	$HOI + RSR \rightarrow NAMS{=}O + I^- + H^+$	125
M10	$I_2 + RSR + H_2O \rightarrow NAMS{=}O + 2H^+ + 2I^-$	5.23
M11	$I_3^- + RSR + H_2O \rightarrow NAMS{=}O + 2H^+ + 3I^-$	1.88

[A]NAMS=O is the sole oxidation product *N*-acetyl-L-methionine sulfoxide.
[B]The units for the forward (k_f) and reverse (k_r) rate constants are determined by reaction molecularity except for where water is involved.

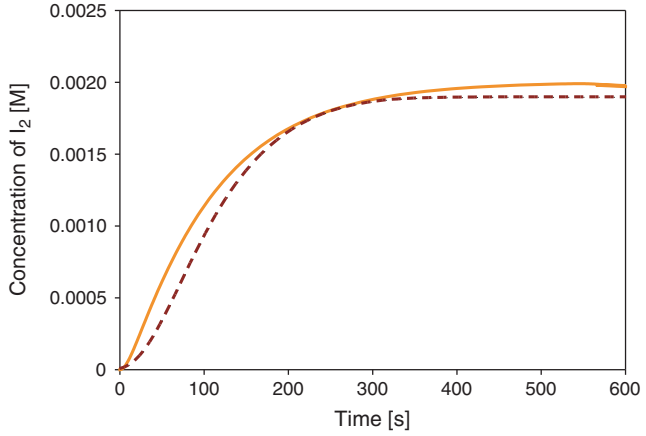

Fig. 15. Computer modelling. Traces showing the simulated results (solid line) and the experimental data (broken line) for data shown in Figs 7–9 and 14 (trace (e)). [*N*-acetyl-L-methionine (NAM)] = 0.01 M, $[IO_3^-] = 0.05$ M, and $[H^+] = 0.006$ M.

concentrations in acidic medium: Reaction M3 lies to the right in acidic medium, and thus very low concentrations of HOI are expected to exist in the highly acidic environments used for these series of studies. k_{M10} was derived from this study, k_{M11} was determined from the best fit for the model. Fig. 15 shows very reasonable agreement between experiments and model for such a simple reaction scheme.

Acknowledgement

This work was supported by Research Grant Number CHE 1056311 from the National Science Foundation.

References

[1] R. B. Freedman, *FEBS Lett.* **1979**, *97*, 201. doi:10.1016/0014-5793(79)80085-X
[2] S. M. Deneke, *Curr. Top. Cell. Regul.* **2001**, *36*, 151. doi:10.1016/S0070-2137(01)80007-8
[3] T. D. Chinevere, R. D. Sawyer, A. R. Creer, R. K. Conlee, A. C. Parcell, *J. Appl. Physiol.* **2002**, *93*, 1590.
[4] J. T. Rotruck, R. W. Boggs, *J. Nutr.* **1975**, *105*, 331.
[5] H. Qavi, S. Kit, *Biochem. Genet.* **1980**, *18*, 669. doi:10.1007/BF00484584
[6] Y. E. Miller, B. Kao, *J. Immunoassay* **1989**, *10*, 129. doi:10.1080/01971528908053232
[7] T. Smith, M. S. Ghandour, P. L. Wood, *J. Neurochem.* **2011**, *118*, 187. doi:10.1111/J.1471-4159.2011.07305.X
[8] R. W. Boggs, J. T. Rotruck, R. A. Damico, *J. Nutr.* **1975**, *105*, 326.
[9] D. H. Baker, *J. Nutr.* **1979**, *109*, 970.
[10] T. T. Daabees, D. W. Andersen, W. L. Zike, L. J. Filer, L. D. Stegink, *J. Nutr.* **1984**, *114*, 1541.
[11] R. W. Boggs, *Adv. Exp. Med. Biol.* **1978**, *105*, 571. doi:10.1007/978-1-4684-3366-1_28
[12] P. E. Ballance, *J. Sci. Food Agric.* **1961**, *12*, 532. doi:10.1002/JSFA.2740120706
[13] K. Lertratanangkoon, J. M. Scimeca, *Toxicol. Appl. Pharmacol.* **1993**, *122*, 191. doi:10.1006/TAAP.1993.1187
[14] L. A. Skoglund, K. Ingebrigtsen, I. Nafstad, O. Aalen, *Biochem. Pharmacol.* **1986**, *35*, 3071. doi:10.1016/0006-2952(86)90388-6
[15] F. Donnarumma, M. Schober, J. Greilberger, V. Matzi, J. Lindenmann, A. Maier, R. Herwig, R. Wintersteiger, *J. Sep. Sci.* **2011**, *34*, 135. doi:10.1002/JSSC.201000574
[16] J. T. Rotruck, R. W. Boggs, *J. Nutr.* **1977**, *107*, 357.
[17] U. Burner, W. Jantschko, C. Obinger, *FEBS Lett.* **1999**, *443*, 290. doi:10.1016/S0014-5793(98)01727-X
[18] R. B. Fox, *J. Clin. Invest.* **1984**, *74*, 1456. doi:10.1172/JCI111558
[19] T. R. Green, J. H. Fellman, A. L. Eicher, *FEBS Lett.* **1985**, *192*, 33. doi:10.1016/0014-5793(85)80037-5
[20] D. B. Learn, V. A. Fried, E. L. Thomas, *J. Leukoc. Biol.* **1990**, *48*, 174.
[21] H. E. Gottlieb, V. Kotlyar, A. Nudelman, *J. Org. Chem.* **1997**, *62*, 7512. doi:10.1021/JO971176V
[22] H. A. Liebhafsky, G. M. Roe, *Int. J. Chem. Kinet.* **1979**, *11*, 693. doi:10.1002/KIN.550110703
[23] T. C. Bruice, A. B. Sayigh, *J. Am. Chem. Soc.* **1959**, *81*, 3416. doi:10.1021/JA01522A066
[24] T. C. Bruice, R. T. Markiw, *J. Am. Chem. Soc.* **1957**, *79*, 3150. doi:10.1021/JA01569A043
[25] S. Carballal, B. Alvarez, L. Turell, H. Botti, B. A. Freeman, R. Radi, *Amino Acids* **2007**, *32*, 543. doi:10.1007/S00726-006-0430-Y
[26] G. Rabai, A. Kaminaga, I. Hanazaki, *J. Phys. Chem.* **1995**, *99*, 9795. doi:10.1021/J100024A021
[27] G. Schmitz, *Phys. Chem. Chem. Phys.* **2000**, *2*, 4041. doi:10.1039/B003606O
[28] Y. Xie, M. R. McDonald, D. W. Margerum, *Inorg. Chem.* **1999**, *38*, 3938. doi:10.1021/IC9807442
[29] G. Schmitz, *Phys. Chem. Chem. Phys.* **1999**, *1*, 1909. doi:10.1039/A809291E
[30] R. Olojo, R. H. Simoyi, *J. Phys. Chem. A* **2004**, *108*, 1018. doi:10.1021/JP036305S
[31] E. Chikwana, B. Davis, M. K. Morakinyo, R. H. Simoyi, *Can. J. Chem.* **2009**, *87*, 689. doi:10.1139/V09-038

[32] J. Pitha, L. Szente, J. Greenberg, *J. Pharm. Sci.* **1983**, *72*, 665. doi:10.1002/JPS.2600720618
[33] K. M. Towle, J. L. Chaytor, H. Liu, P. Austin, M. Roberge, C. D. Roskelley, J. C. Vederas, *Org. Biomol. Chem.* **2013**, *11*, 1476. doi:10.1039/C3OB27238A
[34] D. H. Turner, G. W. Flynn, N. Sutin, J. V. Beitz, *J. Am. Chem. Soc.* **1972**, *94*, 1554. doi:10.1021/JA00760A020
[35] B. S. Yiin, D. W. Margerum, *Inorg. Chem.* **1990**, *29*, 1559. doi:10.1021/IC00333A023
[36] M. Eigen, K. Kustin, *J. Am. Chem. Soc.* **1962**, *84*, 1355. doi:10.1021/JA00867A005
[37] S. Naidich, J. E. Ricci, *J. Am. Chem. Soc.* **1939**, *61*, 3268. doi:10.1021/JA01267A010
[38] N. C. Li, Y.-T. Lo, *J. Am. Chem. Soc.* **1941**, *63*, 394. doi:10.1021/JA01847A014
[39] R. W. Ramette, *J. Chem. Educ.* **1959**, *36*, 191. doi:10.1021/ED036P191